Bioresource Technology 256 (2018) 321–327

Contents lists available at ScienceDirect

Bioresource Technology

journal homepage: www.elsevier.com/locate/biortech

Improving cellulose nanofibrillation of waste wheat straw using the combined methods of prewashing, *p*-toluenesulfonic acid hydrolysis, disk grinding, and endoglucanase post-treatment

Huiyang Bian[a,1], Ying Gao[a,1], Yiqin Yang[a], Guigan Fang[b], Hongqi Dai[a,*]

[a] Jiangsu Co-Innovation Center of Efficient Processing and Utilization of Forest Resources, Nanjing Forestry University, Nanjing 210037, China
[b] China Institute of Chemical Industry of Forestry Products, Chinese Academy of Forestry, Nanjing 210042, China

GRAPHICAL ABSTRACT

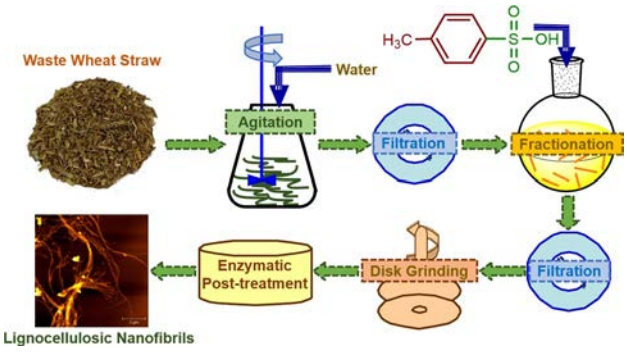

ARTICLE INFO

Keywords:
Waste wheat straw
Prewashing
p-Toluenesulfonic acid hydrolysis
Delignification
Endoglucanase post-treatment
Cellulose nanofibrillation

ABSTRACT

Here we established a new approach for improving the cellulose nanofibrillation of high ash content waste wheat straw (WWS). The results were comprehensively elucidated from the ash removal, delignification, mechanical fibrillation and endoglucanase post-treatment. When water dosage was increased from 50 to 500 times of the WWS weight, the ash content gradually decreased during prewashing process, which facilitated lignin solubilization in subsequent *p*-toluenesulfonic acid (*p*-TsOH) hydrolysis. Approximately 80% of lignin in prewashed WWS could be dissolved during acid hydrolysis to result in a relatively higher crystallinity of 59.1%. Compared with the lignocellulosic nanofibrils (LCNF) directly obtained using acid hydrolysis and disk grinding, prewashing-assisted acid hydrolyzed WWS was fibrillated into LCNF with smaller height of 57.0 nm. Mild endoglucanase post-treatment could further produce less entangled LCNF with thinner diameters. In short, this study presented a promising and green pathway to achieve an efficient utilization of agricultural residue wastes to cellulose nanomaterials.

1. Introduction

Wheat straw (WS), as the most abundant agriculture residues in China, are usually buried in soil or burnt in the field, which may cause air pollution and fire risk (Sanchez et al., 2016). A large scale utilization of wheat straw is necessary to avoid these environmental issues. Wheat

* Corresponding author.
E-mail address: hgdhq@njfu.edu.cn (H. Dai).
[1] These authors contributed equally to this work.

https://doi.org/10.1016/j.biortech.2018.02.038
Received 4 January 2018; Received in revised form 6 February 2018; Accepted 7 February 2018
Available online 10 February 2018
0960-8524/

straw in China is extensively utilized in the pulping industry for extraction of cellulosic materials. However, waste wheat straw (WWS), the solid residue remaining as a byproduct from the wheat straw pulping industry, are difficult to utilize in straw pulp making. It is estimated that the annual generation of the WWS from a Chinese straw pulp mill can be as high as 4×10^5 tons per year (Huang et al., 2017), these residues should be treated for total or at least partial elimination. However, most of the residues are simply burned, representing cost-ineffective usage and potential environmental harm (Tarrés et al., 2017). Developing green and economical pretreatment method for WWS utilization is the key to reap the full benefits of agriculture residues for an environmentally sustainable future.

So far, various approaches have been conducted to produce nanocellulose from WS (Alemdar and Sain, 2008; Barbash et al., 2017; Espinosa et al., 2015; Liu et al., 2017; Shahbazi et al., 2017). These strategies facilitated the effective hydrolysis of hemicellulose and depolymerization of cellulose for subsequent mechanical fibrillation. However, for the successive alkaline and acid pretreatment, the neutralization of chemicals and inability to recycle contributed to the high cost of this method (Alemdar and Sain, 2008). High energy consumption in physic-chemical pretreatment such as ultrasonication and steam explosion composed major challenges in producing nanocellulose with high efficiency and low cost (Barbash et al., 2017; Liu et al., 2017). High demand of reaction temperature and pressure also resulted in high cost and restricted large-scale production (Shahbazi et al., 2017). Most important of all, there are no publicly available studies on the production of WWS nanocellulose, even using the above-mentioned methods.

WWS is mixture of wheat leaves, ears, straw scraps and soil, compared with WS, has more complex chemical components. Considering it relatively high ash and lignin content, an efficient treatment must meet the following requirements: (1) improving the removal of ash and lignin to increase cellulose content of WWS; (2) majority of cellulose can be remained for mechanical fibrillation; (3) obtaining cellulose nanofibrils with uniform diameters and high aspect ratio; (4) the treatment process should be classified as environmentally friendly. Based on the envisaged aim, water prewashing can come to focus as a green method, that is, without addition of chemical additives (Huang et al., 2017). It has been reported that the enzymatic digestibility of WWS was lower than that of prewashed WWS, for which a cellulose hydrolysis yield as high as 84% can be obtained (Huang et al., 2016). Lignin, composed of different kinds of pheylpropane units, is considered to be covalently bonded to the cellulose or hemicellulose, inhibiting enzymatic and acid hydrolysis of lignocelluloses (Bian et al., 2017a; Cai et al., 2016). When using undelignified fibers with lignin content higher than 25%, nanofibrillation became very difficult and fiber suspension sometimes clogged in the reaction chamber (Spence et al., 2010). Therefore, a rapid delignification method should be developed to reduce the lignin content of WWS and protect equipment from clogging during LCNF production. In recent years, disk grinding with SuperMassCollodier (SMC) has received much attention for its potential in nanocellulose scale-up. However, the CNF obtained through SMC appeared to be less homogeneous in terms of fibril diameters, compared with CNF produced by homogenization or microfluidization. In order to reduce non-uniformity in the diameters of the fibrils produced by mechanical fibrillation, enzymatic post-treatment was more attractive due to the environmentally friendly reaction conditions (Wang et al., 2016).

Here, a new pathway for improving the cellulose nanofibrillation of waste wheat straw (WWS) was reported. Prewashing treatment was firstly carried out to reduce the free ash content in the WWS, delignification process was then processed using an aromatic acid, *p*-toluenesulfonic acid (*p*-TsOH), which has been used for enzymatic saccharification (Amarasekara and Wiredu, 2012; Ji et al., 2017), furfural production (Ji et al., 2016), wood fractionation (Chen et al., 2017) and lignocellulose nanomaterials production (Bian et al., 2017b). The aim of prewashing and *p*-TsOH acid hydrolysis is to remove ash, separate lignin and depolymerize cellulose, thereby making straw pulping residue a valuable product lignocellulosic nanofibrils (LCNF) in the disk grinding process. The endoglucanase post-treatment can further improve cellulose nanofibrillation, producing the desired fibril diameter to meet the market demands for LCNF. Compared with many existing treatment technologies, we believe that this work provides useful information in comprehensive utilization of agricultural residue wastes.

2. Materials and methods

2.1. Materials

The WWS used in the work was provided from a straw pulp mill in LiaoCheng, Shandong, China. *p*-Toluenesulfonic acid (*p*-TsOH) was analytical reagent and purchased from LiFeng Chemical Reagent Co. Ltd., Shanghai. Dialysis bags with a typical cut-off molecular weight of 14 kDa were obtained from Sigma-Aldrich (Product No. D9402-100FT). Cellulase (Celluclast 1.5L) was kindly provided by Novozymes Biotechnology Co. Ltd (Guangzhou, China). The cellulase activity of Celluclast 1.5L was 753.52 endoglucanase units (EGU)/g. Filter paper (15 cm, slow) was from Fisher Scientific Inc. (Pittsburgh, PA).

2.2. Prewashing treatment

Prior to the acid hydrolysis, the WWS was washed with deionized (DI) water to remove the free ash. The prewashing treatment of the WWS was conducted in different solid to liquid ratios, equal to 1:50, 1:200, and 1:500, and the prewashed WWS were abbreviated to WWS50, WWS200, and WWS500, respectively. WWS of 20 g (in dry weight) was soaked in the required amounts of DI water using a Homo Disper at 600 rpm for 15 min. The mixture was then pressed with a cloth bag to remove the washing water. All prewashed WWS were oven dried at 40 °C overnight and stored in plastic bags.

2.3. Fractionation using p-TsOH

Acid hydrolysis was conducted in 80% (w/w) concentration *p*-TsOH acid solution at 80 °C for 20 min, as described previously (Bian et al., 2017b). The *p*-TsOH acid solution was prepared by mixing acid and DI water in a three-necked flask, then heated to 80 °C in a water bath. Original or prewashed WWS of 10 g (oven dry weight) was manually fed into the completely dissolved acid solution, resulting in a liquor to solid mass ratio of 10:1. The suspension was constantly agitated using a mechanical mixer at 300 rpm. At the end of each reaction, 100 mL of DI water was added to quench the reaction. The hydrolysate was then separated by vacuum filtration through a filter paper. Because *p*-TsOH only acted as a catalyst and has a low water solubility at ambient temperature. Efficient recovery can be accomplished using crystallization technology by cooling re-concentrated spent acid solution to achieve environmental sustainability. The filter cake was further washed using DI water and collected for chemical composition analysis and LCNF production. The hydrolyzed samples were given label designations of HWWS, HWWS50, HWWS200, and HWWS500 (seen in Table 1).

2.4. Mechanical nanofibrillation

All hydrolyzed samples were mechanically fibrillated for producing LCNF using a stone disk grinder SuperMassCollodier (SMC) (Model: MKCA6-2J, Disk Model: MKG-C, Masuko Sangyo Co., Ltd, Japan) at solids loading of 1% (w/w) at 1500 rpm (Qin et al., 2016). Initially, the disk gap was dynamically set to zero (two disks just touch each other) without pulp. Then, with the addition of pulp, the gap was adjusted down to −150 μm. Due to the presence of pulp suspension or slurry, there was no direct contact between the two grinding disks even with a negative clearance. Fiber suspension was fed by gravity continuously

Table 1
Chemical compositions of prewashed WWS and *p*-TsOH hydrolyzed prewashed WWS.

Sample Label	Cellulose (%)	Hemicellulose (%)		Lignin (%)		Ash (%)	Hydrolysis yield (%)
		Xylan (%)	Arabinan (%)	Acid-soluble lignin (%)	Klason lignin (%)		
WWS	24.28 ± 0.01	11.89 ± 0.66	2.47 ± 0.01	2.42 ± 0.02	16.14 ± 1.17	35.30 ± 0.89	100
HWWS	25.36 ± 2.81	7.22 ± 1.03	1.15 ± 0.04	0.83 ± 0.01	18.82 ± 0.24	48.05 ± 2.55	55.9
WWS50	29.26 ± 1.26	13.15 ± 0.37	3.49 ± 0.49	2.50 ± 0.47	17.63 ± 0.57	21.94 ± 0.22	100
HWWS50	45.89 ± 2.24	5.66 ± 0.40	0.38 ± 0.36	0.98 ± 0.01	12.95 ± 0.93	28.52 ± 0.87	54.8
WWS200	32.34 ± 0.22	18.16 ± 1.12	3.17 ± 0.18	2.69 ± 0.05	22.49 ± 0.64	12.82 ± 0.51	100
HWWS200	42.68 ± 1.49	4.62 ± 0.16	0.21 ± 0.08	0.94 ± 0.09	12.45 ± 1.22	20.27 ± 1.13	45.7
WWS500	33.49 ± 0.76	19.16 ± 0.46	3.46 ± 0.26	2.40 ± 0.45	22.91 ± 0.40	9.62 ± 0.64	100
HWWS500	49.19 ± 1.46	5.35 ± 1.11	0.60 ± 0.49	1.25 ± 0.01	8.79 ± 0.25	15.35 ± 1.31	45.4

through a hopper and collected using a plastic beaker. The fibrillated suspension was discharged by centrifugal force, and passed through the disk chamber for 5 times.

2.5. Endoglucanase post-treatment

LCNFs produced by SMC were further post-treated using endoglucanase (Celluclast 1.5L). Endoglucanase post-treatment was performed with a working volume of 50 mL in 250 mL flasks with a substrate loading of 1% (w/v) at 50 °C, pH 4.8 and 150 rpm for 8 h. The endoglucanase loading in the experiments were all 30 mg/g cellulose. Endoglucanases were denatured at the end of post-treatment by incubating in boiling water for 20 min. The resultant endoglucanase post-treated lignocellulosic nanofibrils (E-LCNF) were stored at 4 °C for further analysis. A schematic flow diagram describing the combined methods for improving cellulose nanofibrillation of WWS is shown in Fig. 1.

2.6. Chemical composition analyses

The chemical compositions of raw WWS, prewashed WWS and acid hydrolyzed samples were determined using the procedure proposed by National Renewable Energy Laboratory (NREL), specifically including cellulose, xylan, arabinan, lignin and ash (Sluiter et al., 2008a,b). The lignin remaining rate in residual solids after acid hydrolysis, L_R, can be determined from the measured lignin content of initial and residual solid, and hydrolysis yield. The calculation Eqs. (1) and (2) were listed as follows:

$$\text{Hydrolysis yield (\%)} = \frac{\text{Residual solid (g)}}{\text{Initial material (g)}} \times 100 \quad (1)$$

$$\text{Lignin remaining rate } (L_R) = \frac{(1) \times \text{Lignin content in residual solid (\%)}}{\text{Lignin content in initial material (\%)}} \quad (2)$$

2.7. Morphology observation

The morphologies of the original WWS and acid hydrolyzed samples were observed using scanning electron microscopy (SEM). Samples were sputter-coated with gold to provide adequate conductivity. Images were observed and recorded using a SEM system (Quanta 200, FEI, USA). The morphologies of LCNF and E-LCNF were analyzed by atomic force microscopy (AFM; Dimension Edge, Bruker, Germany). Samples were diluted to solids consistency of 0.01 wt% and deposited onto clean mica substrates and air dried overnight at room temperature. AFM topographical images were obtained in tapping mode at 300 kHz using a standard silicon cantilever and a tip with radius of curvature of 8 nm. Fibril height distribution was measured using Gwyddion software (Department of Nanometrology, Czech Metrology Institute, Crezh Republic, 64-bit).

2.8. X-ray diffraction (XRD)

The XRD patterns were measured using an Ultima IV diffractometer at a voltage of 40 kV and a current of 30 mA (Rigaku Corp., Tokyo, Japan). Scattering radiation was detected in a 2θ range from 10° to 40° in steps of 0.02°. The crystallinity index (CrI) was calculated using the Eq. (3) in accordance with the Segal method (without baseline substrate) (Segal et al., 1959):

$$\text{CrI} = \frac{I_{002} - I_{am}}{I_{002}} \times 100\% \quad (3)$$

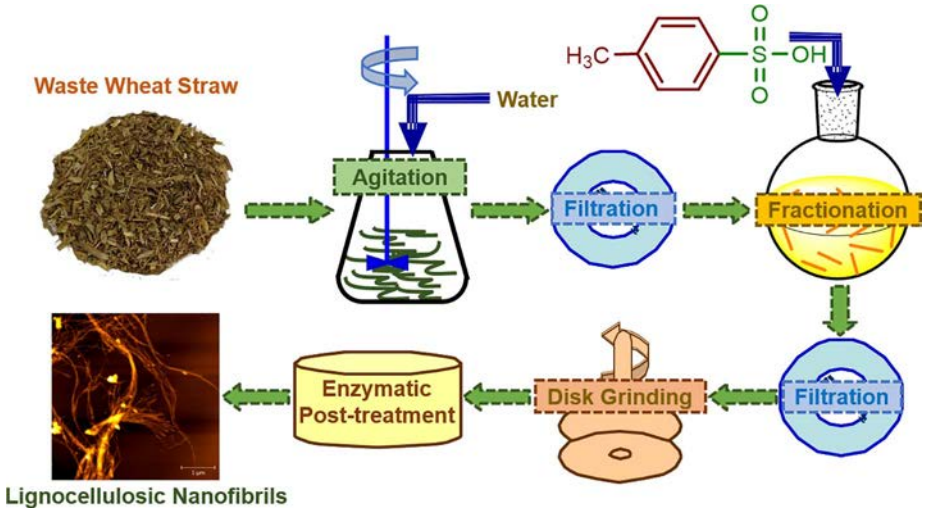

Fig. 1. A schematic flow diagram describing the combined methods for improving cellulose nanofibrillation of waste wheat straw.

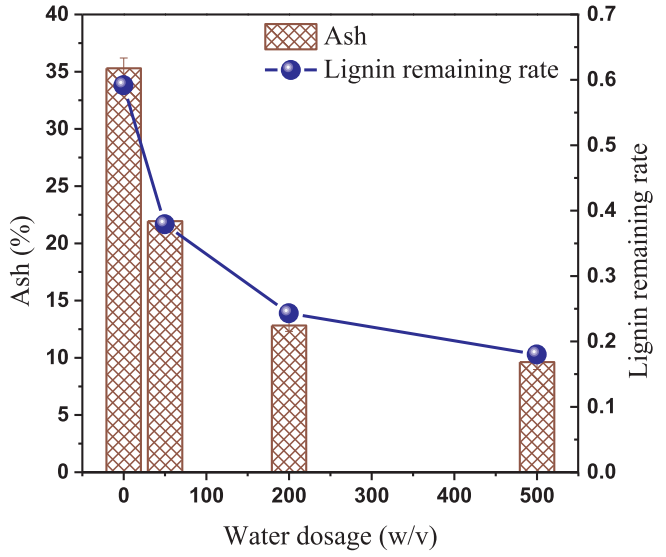

Fig. 2. Effects of water dosage on the ash content of prewashed WWS and lignin remaining rate of residual solids after acid hydrolysis.

where I_{002} is the maximum peak intensity at a 2θ angle close to 22.5°, and I_{am} is the minimum diffraction intensity at a 2θ angle close to 18°.

3. Results and discussion

3.1. Effects of prewashing on chemical compositions of WWS and HWWS

The chemical composition changes of prewashed WWS and *p*-TsOH hydrolyzed prewashed WWS were listed in Table 1. For comparison purpose the result from WWS was also presented. Because WWS was considered as complicated materials, containing wheat leaves, ears and straw scraps, as well as a lot of soil, cellulose content was only 24.28%, lower than conventional wheat straw with cellulose content of 35.60%. Therefore, the ash contents of WWS were considerably higher than that of wheat straw. In order to relieve the influence of ash in the WWS on the pretreatment, water washing process was introduced prior to *p*-TsOH hydrolysis. As can be seen in Fig. 2, when the water dosage of the prewashing process was increased from 50 to 500 times of the WWS weight, the ash content of prewashed WWS decreased from 35.30% to 9.62%, thus increasing the carbohydrates content of the prewashed WWS. It should be noted that 9.62% of the ash could not be completely removed in HWWS500 even after prewashing with large amounts of water, this residual ash could be mainly structural, which cannot be easily removed by water washing, in agreement with a previous study (Huang et al., 2016).

To evaluate the effects of prewashing on the acid hydrolysis efficiency of WWS, the chemical composition and yield of *p*-TsOH hydrolyzed samples were also determined (Table 1). The results indicated that the prewashing process enhanced the acid hydrolysis efficiency of pretreated WWS, in which the yield of residual solid was decreased from 55.9% to 45.4%. The same tendency was obtained in the lignin remaining rate, which decreased from 0.59 to 0.18 (Fig. 2), suggesting that approximately 80% of WWS lignin could be dissolved after *p*-TsOH acid hydrolysis when the washing water was equal to 500 times of WWS weight. As a strong organic acid, *p*-TsOH can easily donate a proton in an aqueous solution to isolate lignin by breaking glycosidic, ether and ester bonds in carbohydrates, lignin, and lignin-carbohydrate complexes (Chen et al., 2017). However, free ash in WWS might neutralize the acidic catalysts, resulting in invalid consuming of a substantial amount of acid. Prewashing destroyed the buffering effect of free ash, and in turn enhanced the acid hydrolysis and delignification efficiency. The great selectivity of solubilizing lignin over the dissolution of cellulose will be beneficial for the downstream LCNF production.

3.2. Effects of prewashing on the crystallinity of HWWS

It is generally known that crystallinity has been recognized as one of the major substrate properties determining hydrolysis rate. In this work, the amorphous fraction of WWS could be related to hemicellulose, lignin and ash, and cellulose was almost considered crystallinity. The XRD analysis results presented that SiO_2, $KAlSi_2O_3$, $CaAl_2Si_2O_8$ and $CaCO_3$ were the major component from WWS ashes (Wang et al., 2017). XRD measurements also indicated that WWS as well as HWWS500 have two characteristic peaks at about 16.4° and 22.6°, corresponding to the (1 1 0) and (2 0 0) reflection planes of typical cellulose I structure, respectively, revealing that prewashing and acid hydrolysis did not destroy or alter the inherent crystal structure of cellulose (Lin and Dufresne, 2014). And the prewashing-assisted acid hydrolysis increased CrI of WWS from 50.1 to 59.1%. Based on the above chemical composition and XRD patterns analyses, it could be concluded that prewashing removed large amounts of ashes and *p*-TsOH hydrolysis dissolved substantial amounts of amorphous lignin. Recall, 9.62% of ash were retained in prewashed WWS. These structural components could not be dissolved even after hydrolyzing with concentrated acid and mainly existed in the form of SiO_2.

3.3. Morphologies of WWS and HWWS

The morphological changes caused by prewashing and *p*-TsOH hydrolysis were examined using SEM to obtain insights into the structure in WWS. Due to the cellulose depolymerization, the acid hydrolyzed WWS were shortened compared with the raw WWS. It was apparent that disrupted fiber surface morphology and irregular particles could be observed after acid hydrolysis. The formed particles could be attributed to the presence of ash or lignin in WWS. Moreover, the fiber shortening was less pronounced for HWWS than HWWS500 due to the higher ash content in WWS that impeded cellulose degradation during acid hydrolysis. However, concentrated *p*-TsOH acid hydrolysis could only produce very low yield of crystal-like cellulose nanomaterials, or CNC, which were often isolated after dialyzing hydrolyzed solid when using concentrated mineral acids or other organic acids (Chen et al., 2016). Thus, it seemed that the prewashing-assisted acid hydrolysis treatment could mainly remove ash and lignin, but not the cellulose in WWS.

3.4. Effects of prewashing on the nanofibrillation efficiency of HWWS

The acid hydrolyzed samples were subsequently mechanical fibrillated into LCNF. The morphology of SMC fibrillated LCNF varied with the severity of prewashing treatment as shown by AFM images. Increasing the prewashing severity (or water weight) resulted in less entangled LCNF with thinner diameters as shown from the AFM measured height distribution (Fig. 3). The mean LCNF fibril height decreased from 152.7 to 121.8, 82.9 and 57.0 nm, when the dosage of water was increased by 50, 200 and 500 times, respectively. The residual lignin and ash contents of these hydrolyzed samples were 66.9, 41.5, 32.8 and 24.1%, respectively, for HWWS, HWWS50, HWWS200 and HWWS500. Furthermore, the distribution became narrower or more uniform as the lignin and ash content decreased. These results suggested that higher lignin and ash content impeded mechanical fibrillation. Our previous study reported three LCNF samples of

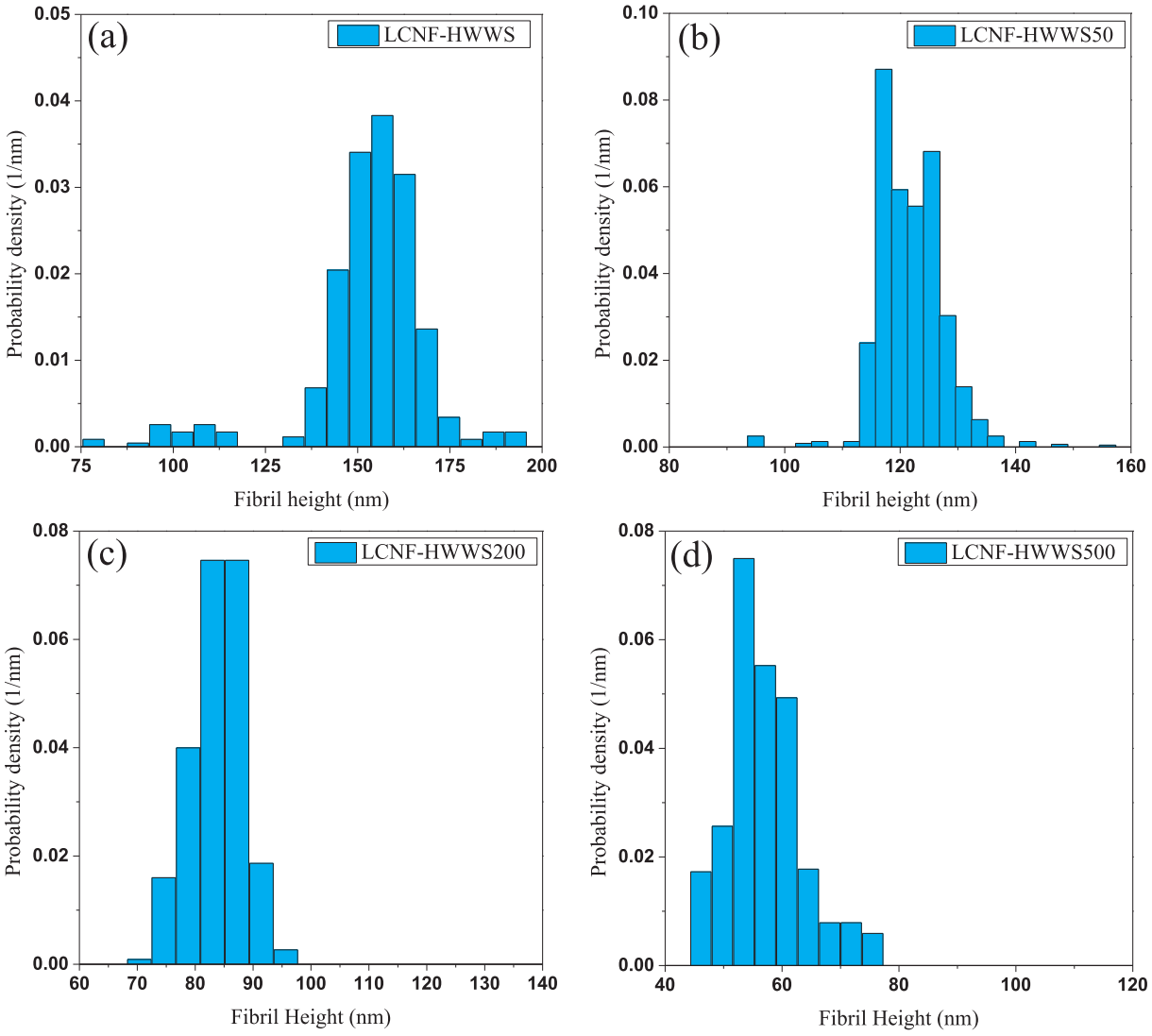

Fig. 3. AFM measured height probability density distributions of the lignocellulosic nanofibrils (LCNF). (a) LCNF-HWWS; (b) LCNF-HWWS50; (c) LCNF-HWWS200; (d) LCNF-HWWS500.

approximately 51.1, 29.4 and 15.3 nm in height (Bian et al., 2017b). These LCNF samples were produced using the same concentrated *p*-TsOH acid hydrolysis of medium density fiberboard of lignin content 16.0, 11.6 and 7.18%, respectively. In this work, lignin and ash in WWS were suggested to impede mechanical nanofibrillation due to their larger size compared with cellulose after acid hydrolysis. Prewashing process not only enhanced the removal the free ash, but also improved the delignification efficiency of WWS, thus facilitating cellulose nanofirbillation in disk grinding process.

3.5. Effects of endoglucanase post-treatment on the nanofibrillation efficiency of the resulting LCNF

The morphologies of E-LCNF were observed using AFM images. It was apparent that more uniform nanofibril morphology could be obtained after endoglucanase post-treatment. Endoglucanase cleaved β-1,4 linkages of cellulose, which created new chain ends and reduced cellulose chain length (Wang et al., 2016), resulting in E-LCNF with smaller diameters and shorter lengths. Furthermore, the fibril height distribution of E-LCNF became narrower or more uniform as the endoglucanase was added (Fig. 4). These results suggested that endoglucanase promoted cellulose nanofibrillation, in agreement with a previous study (Long et al., 2017). To further illustrated this, number-average fibril heights of the LCNF and E-LCNF were calculated and compared in Fig. 5. The mean fibril heights were 116.5, 84.2, 44.0 and 37.3 nm, respectively, for E-LCNF-HWWS, E-LCNF-WWS50, E-LCNF-WWS200 and E-LCNF-HWWS500, lower than corresponding LCNF without endoglucanase post-treatment. According to fibril morphology and heights, endoglucanase worked the best on E-LCNF-HWWS500 compared with other E-LCNF samples based on fibril size uniformity. This was due to the fact that lignin and ash in WWS were considered to be the inhibitors to reduce enzymatic hydrolysis efficiency and limit excess cellulose nanofibrillation. The inhibition effect of free ash and lignin on the endoglucanase post-treatment were removed by prewashing and acid hydrolysis, thus obtaining uniform-sized E-LCNF with higher aspect ratio. Based on the above-mentioned discussions, the combined method using prewashing, *p*-TsOH hydrolysis, disk grinding and endoglucanase post-treatment is an effective approach to improve cellulose nanofibrillation of WWS in LCNF production.

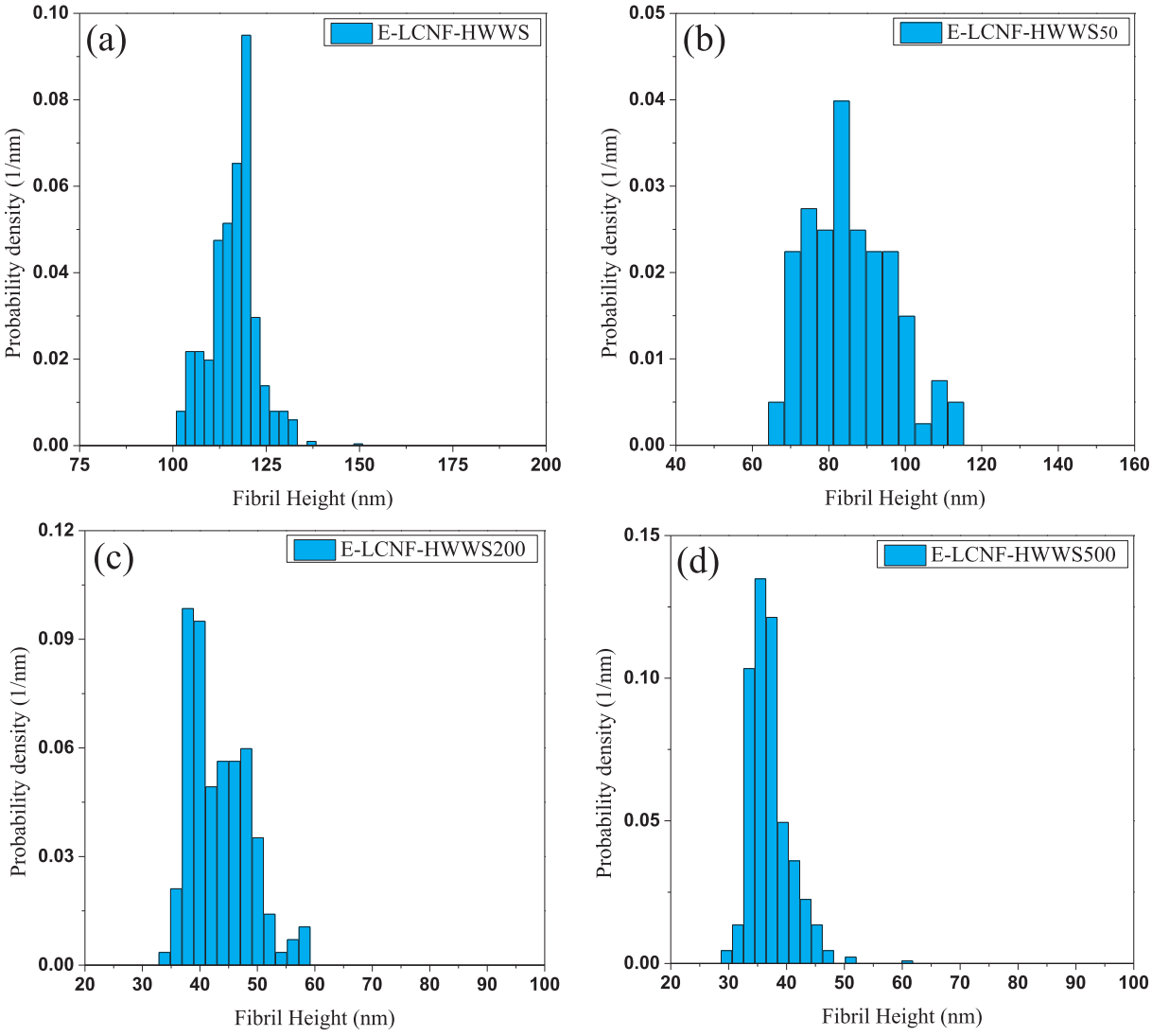

Fig. 4. AFM measured height probability density distributions of the endoglucanase post-treated lignocellulosic nanofibrils (E-LCNF). (a) E-LCNF-HWWS; (b) E-LCNF-HWWS50; (c) E-LCNF-HWWS200; (d) E-LCNF-HWWS500.

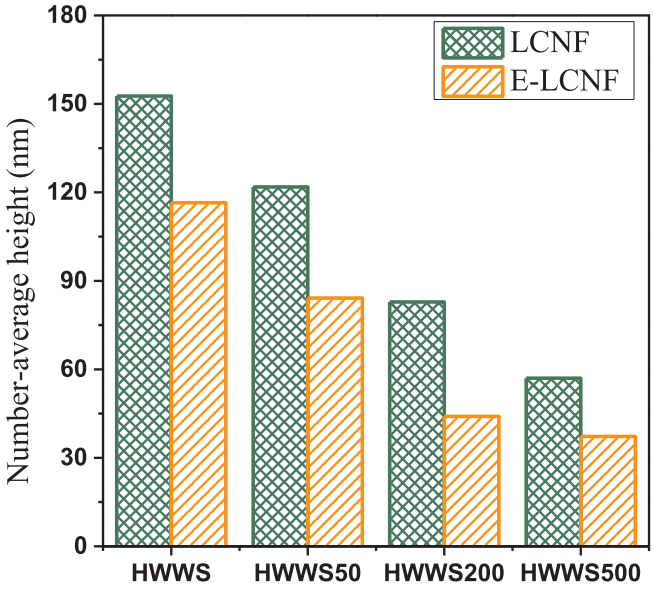

Fig. 5. Comparisons of the number-average fibril height of the LCNF and E-LCNF.

4. Conclusion

This study developed a novel method to improve cellulose nanofibrillation of WWS. Prewashing treatments with different water dosage were employed to remove free ash. Up to 80% lignin in WWS was rapidly solubilized in subsequent *p*-TsOH hydrolysis. The hydrolyzed WWS fiber with lignin content of 8.8% could be mechanically fibrillated to produce LCNF with average height of 57.0 nm. Endoglucanase post-treatment was finally performed to obtain a more uniform LCNF with average height of 37.3 nm. The process we presented can be a promising approach for high value utilization of agricultural residue wastes.

Acknowledgements

This work was financially supported from the National Natural Science Foundation of China (Project No. 31470599) and the Doctorate Fellowship Foundation of Nanjing Forestry University. The authors also thank Jing Yang and Buhong Gao of Nanjing Forestry University for SEM and AFM analyses, respectively.

Appendix A. Supplementary data

Supplementary data associated with this article can be found, in the online version, at http://dx.doi.org/10.1016/j.biortech.2018.02.038.

References

Alemdar, A., Sain, M., 2008. Isolation and characterization of nanofibers from agricultural residues: wheat straw and soy hulls. Bioresour. Technol. 99, 1664–1671.

Amarasekara, A.S., Wiredu, B., 2012. A comparison of dilute aqueous p-toluenesulfonic and sulfuric acid pretreatments and saccharification of corn stover at moderate temperatures and pressures. Bioresour. Technol. 125, 114–118.

Barbash, V.A., Yaschenko, O.V., Shniruk, O.M., 2017. Preparation and properties of nanocellulose from organosolv straw pulp. Nanoscale Res. Lett. 12, 241.

Bian, H., Chen, L., Dai, H., Zhu, J.Y., 2017a. Integrated production of lignin containing cellulose nanocrystals (LCNC) and nanofibrils (LCNF) using an easily recyclable dicarboxylic acid. Carbohydr. Polym. 167, 167–176.

Bian, H., Chen, L., Gleisner, R., Dai, H., Zhu, J.Y., 2017b. Producing wood-based nanomaterials by rapid fractionation of wood at 80 °C using a recyclable acid hydrotrope. Green Chem. 19, 3370–3379.

Cai, C., Qiu, X., Lin, X., Lou, H., Pang, Y., Yang, D., Chen, S., Cai, K., 2016. Improving enzymatic hydrolysis of lignocellulosic substrates with pre-hydrolysates by adding cetyltrimethylammonium bromide to neutralize lignosulfonate. Bioresour. Technol. 216, 968–975.

Chen, L., Dou, J., Ma, Q., Li, N., Wu, R., Bian, H., Yelle, D.J., Vuorinen, T., Fu, S., Pan, X., Zhu, J.Y., 2017. Rapid and near-complete dissolution of wood lignin at ≤80°C by a recyclable acid hydrotrope. Sci. Adv. 3, e1701735.

Chen, L., Zhu, J.Y., Baez, C., Kitin, P., Elder, T., 2016. Highly thermal-stable and functional cellulose nanocrystals and nanofibrils produced using fully rrecyclable organic acids. Green Chem. 18, 3835–3843.

Espinosa, E., Tarrés, Q., Delgado-Aguilar, M., González, I., Mutjé, P., Rodríguez, A., 2015. Suitability of wheat straw semichemical pulp for the fabrication of lignocellulosic nanofibres and their application to papermaking slurries. Cellulose 23, 837–852.

Huang, C., Lai, C., Wu, X., Huang, Y., He, J., Huang, C., Li, X., Yong, Q., 2017. An integrated process to produce bio-ethanol and xylooligosaccharides rich in xylobiose and xylotriose from high ash content waste wheat straw. Bioresour. Technol. 241, 228–235.

Huang, C., Wu, X., Huang, Y., Lai, C., Li, X., Yong, Q., 2016. Prewashing enhances the liquid hot water pretreatment efficiency of waste wheat straw with high free ash content. Bioresour. Technol. 219, 583–588.

Ji, H., Chen, L., Zhu, J.Y., Gleisner, R., Zhang, X., 2016. Reaction kinetics based optimization of furfural production from corncob using a fully recyclable solid acid. Ind. Eng. Chem. Res. 55, 11253–11259.

Ji, H., Song, Y., Zhang, X., Tan, T., 2017. Using a combined hydrolysis factor to balance enzymatic saccharification and the structural characteristics of lignin during pretreatment of Hybrid poplar with a fully recyclable solid acid. Bioresour. Technol. 238, 575–581.

Lin, N., Dufresne, A., 2014. Surface chemistry, morphological analysis and properties of cellulose nanocrystals with gradiented sulfation degrees. Nanoscale 6, 5384–5393.

Liu, Q., Lu, Y., Aguedo, M., Jacquet, N., Ouyang, C., He, W., Yan, C., Bai, W., Guo, R., Goffin, D., Song, J., Richel, A., 2017. Isolation of high-purity cellulose nanofibers from wheatstraw through the combined environmentally friendly methods of steam explosion, microwave-assisted hydrolysis, and microfluidization. ACS Sustain. Chem. Eng. 5, 6183–6191.

Long, L., Tian, D., Hu, J., Wang, F., Saddler, J., 2017. A xylanase-aided enzymatic pretreatment facilitates cellulose nanofibrillation. Bioresour. Technol. 243, 898–904.

Qin, Y.L., Qiu, X.Q., Zhu, J.Y., 2016. Understanding longitudinal wood fiber ultrastructure for producing cellulose nanofibrils using disk milling with diluted acid prehydrolysis. Sci. Rep. 6, 35602.

Sanchez, R., Espinosa, E., Dominguez-Robles, J., Loaiza, J.M., Rodriguez, A., 2016. Isolation and characterization of lignocellulose nanofibers from different wheat straw pulps. Int. J. Biol. Macromol. 92, 1025–1033.

Segal, L., Creely, J.J., Martin, A.E., Conrad, C.M., 1959. An empirical method for estimating the degree of crystallinity of native cellulose using the X-ray diffractometer. Text. Res. J. 29, 786–794.

Shahbazi, P., Behzad, T., Heidarian, P., 2017. Isolation of cellulose nanofibers from poplar wood and wheat straw: optimization of bleaching step parameters in a chemo-mechanical process by experimental design. Wood Sci. Technol. 51, 1173–1187.

Sluiter, A., Hames, B., Ruiz, R., Scarlata, C., Sluiter, J., Templeton, D., 2008a. Determination of ash in biomass. NREL Chemical Analysis and Testing Laboratory Analytical Procedures. NREL, Golden CO NREL/TP-510-42622.

Sluiter, A., Hames, B., Ruiz, R., Scarlata, C., Sluiter, J., Templeton, D., 2008b. Determination of structural carbohydrates and lignin in biomass. NREL Chemical Analysis and Testing Laboratory Analytical Procedures. NREL, Golden CO NREL/TP-510-42618.

Spence, K.L., Venditti, R.A., Habibi, Y., Rojas, O.J., Pawlak, J.J., 2010. The effect of chemical composition on microfibrillar cellulose films from wood pulps: mechanical processing and physical properties. Bioresour. Technol. 101, 5961–5968.

Tarrés, Q., Espinosa, E., Domínguez-Robles, J., Rodríguez, A., Mutjé, P., Delgado-Aguilar, M., 2017. The suitability of banana leaf residue as raw material for the production of high lignin content micro/nano fibers: from residue to value-added products. Ind. Crop. Prod. 99, 27–33.

Wang, W.X., Mozuch, M.D., Sabo, R.C., Kersten, P., Zhu, J.Y., Jin, Y.C., 2016. Endoglucanase post-milling treatment for producing cellulose nanofibers from bleached eucalyptus fibers by a supermasscolloider. Cellulose 23, 1859–1870.

Wang, Y., Tan, H., Wang, X., Du, W., Mikulčić, H., Duić, N., 2017. Study on extracting available salt from straw/woody biomass ashes and predicting its slagging/fouling tendency. J. Clean. Prod. 155, 164–171.